Proton inhibition of unitary currents of vanilloid receptors

Beiying Liu,[1] Jing Yao,[1] Yingwei Wang,[2] Hui Li,[1] and Feng Qin[1]

[1]Department of Physiology and Biophysical Sciences, State University of New York at Buffalo, Buffalo, NY 14214
[2]Department of Anesthesiology, Xinhua Hospital, Shanghai Jiaotong University School of Medicine, Shanghai 200092, China

Protons, which are released during inflammation and injury, regulate many receptors and ion channels involved in pain transduction, including capsaicin channels (transient receptor potential vanilloid receptors 1). Whereas extracellular acidification both sensitizes and directly activates the channel, it also causes concomitant reduction of the unitary current amplitudes. Here, we investigate the mechanisms and molecular basis of this inhibitory effect of protons on channel conductance. Single-channel recordings showed that the unitary current amplitudes decreased with extracellular pH in a dose-dependent manner, consistent with a model in which protons bind to a site within the channel with an apparent pKa of ~6. The inhibition was voltage dependent, ~65% at −60 mV and 37% at +60 mV when pH was reduced from 7.4 to 5.5. The unitary current amplitudes reached saturation at $[K^+] \geq 1$ M, and notably the maximum amplitudes did not converge with different pHs, inconsistent with a blockade model based on surface charge screening or competitive inhibition of permeating ions. Mutagenesis experiments uncovered two acidic residues critical for proton inhibition, one located at the pore entrance and the other on the pore helix. Based on homology to the KcsA structure, the two acidic residues, along with another basic residue also on the pore helix, could form a triad interacting with each other through extensive hydrogen bonds and electrostatic contacts, suggesting that protons may mediate the interactions between the selectivity filter and pore helix, thereby altering the local structure in the filter region and consequently the conductance of the channel.

INTRODUCTION

Protons are important mediators for pain transduction. Intracutaneous infusion of acidic solutions in humans induces long-lasting pricking and burning pain (Steen and Reeh, 1993; Steen et al., 1996; Ugawa et al., 2002; Jones et al., 2004). Tissue acidosis, which is accompanied with inflammation, arthritis, ischemia, angina, or cancer, is believed to contribute to the pain experienced under these conditions (Issberner et al., 1996; Stoop et al., 1997; Chen et al., 1998; Pan et al., 1999; Sutherland et al., 2001; Garber, 2003). In isolated primary afferents, acidification of extracellular solutions activates multiple types of cationic currents (Krishtal and Pidoplichko, 1981; Bevan and Yeats, 1991; Baumann et al., 1996; Waldmann et al., 1997; Tominaga et al., 1998), among which transient receptor potential vanilloid receptor subtype 1 (TRPV1) is thought to mediate the slowly desensitizing components. Neurons from mice lacking TRPV1 exhibit strongly reduced proton sensitivity (Caterina et al., 2000; Davis et al., 2000), supporting a role for the channel in acid-induced pain syndromes.

Protons exert several effects on TRPV1 functions. Moderate extracellular acidification sensitizes its responses to other stimuli, such as capsaicin and heat, causing them to elicit pain at conditions that are otherwise non-noxious (Petersen and LaMotte, 1993; Martenson et al., 1994; Baumann et al., 1996; Kress et al., 1996; Caterina et al., 1997; Tominaga et al., 1998). Severe acidification leads to direct activation of the channel (Bevan and Yeats, 1991; Baumann et al., 1996; Tominaga et al., 1998). Besides gating effects, extracellular protons also cause reduction of the unitary conductance of the channel (Baumann and Martenson, 2000; Ryu et al., 2003). Moreover, activation of TRPV1 results in intracellular acidification in nociceptive neurons, suggesting that protons may also enter cells through the channel (Hellwig et al., 2004). There have been extensive studies on the mechanisms and structural basis of proton-mediated gating effects (Jordt et al., 2000; Ryu et al., 2003, 2007). In contrast, the conductance effects of protons have not been well understood.

Protons decrease the conductance of a variety of ion channels, such as Na^+ (Begenisich and Danko, 1983; Zhang and Siegelbaum, 1991; Daumas and Andersen, 1993; Bénitah et al., 1997), Ca^{2+} (Tytgat et al., 1990; Klöckner and Isenberg, 1994; Chen et al., 1996), CNG (Root and MacKinnon, 1994; Morrill and MacKinnon, 1999), and K^+ channels (Davies et al., 1992; Coulter et al., 1995; Lopes et al., 2000; Xu et al., 2000; Geiger et al., 2002; Nimigean et al., 2003; Brelidze and Magleby, 2004). Three common models have been proposed to account

B. Liu, J. Yao, and Y. Wang contributed equally to this paper.
Correspondence to Feng Qin: qin@buffalo.edu

Abbreviation used in this paper: TRPV1, transient receptor potential vanilloid receptor subtype 1.

The Rockefeller University Press $30.00
J. Gen. Physiol. Vol. 134 No. 3 243–258
www.jgp.org/cgi/doi/10.1085/jgp.200910255

for the reduction of currents by protons. Early studies in sodium channels indicate that the current reduction by protons is voltage dependent, leading to the suggestion that protons bind to sites within the transmembrane electric field to block ion flow (Woodhull, 1973). Voltage-independent inhibition of sodium current by protons was also observed, prompting the second hypothesis that the apparent voltage-dependent block of current is due to a proton-dependent modification of channel gating (Campbell, 1982). Third, protons may titrate external negative charges to reduce local ionic concentrations near channels (Drouin and Neumcke, 1974). Recently, protons are shown to bind competitively with K^+ ions in BK channels (Brelidze and Magleby, 2004). In L-type Ca^{2+}, CNG, and Kir1.1 channels, proton binding is found to involve negatively charged glutamate residues lying on the ion conduction pathway (Chen et al., 1996; Morrill and MacKinnon, 1999; Xu et al., 2000). Titration of these residues leads to partial or complete blockade of channel conductance.

Here, we examined proton inhibition of single-channel conductance of TRPV1. We found that the reduction of the unitary current amplitudes by protons was inadequately accounted for by conventional models, such as the Woodhull model or those based on surface charge screening. In particular, at saturating ionic concentrations, the unitary current amplitudes did not converge with different extracellular pHs. By mutagenesis experiments, we identified two acidic residues responsible for the proton effects, one at the pore entrance and the other on the pore helix. Based on these results, we suggest that the apparent inhibition of the conductance by protons in TRPV1 may be associated with local structural perturbations in the outer pore region due to altered interactions between the pore helix and the vestibular wall or the selectivity filter.

MATERIALS AND METHODS

Mutagenesis and expression

The plasmid containing the wild-type rat TRPV1 was provided by D. Julius (University of California, San Francisco, San Francisco, CA) (Caterina et al., 1997). Mutations were generated using the overlap extension PCR method as described previously (Liu et al., 2004). The products of the recombinant constructs were confirmed by restriction enzyme digestion and by DNA sequencing. Capped cRNA was synthesized using the mMessage mMachine kit (Applied Biosystems). The final cRNA was resuspended in RNase-free water to ~1 ng/nl and stored at −80°C.

Xenopus laevis oocytes were isolated enzymatically as described previously (Hui et al., 2003) and hand selected 1 or 2 d after harvesting for microinjection of cRNA. Typically, each oocyte received 10–30 ng cRNA. The injected oocytes were incubated in ND96 solution supplemented with 2.5 mM sodium pyruvate, 100 U penicillin per ml, and 100 µg streptomycin per ml at 18°C for 1–2 d. The vitelline layer of injected oocytes was manually removed before patch clamp recording.

HEK293 cells were grown in Dulbecco's modified Eagle's medium containing 10% fetal bovine serum (Hyclone Laboratories, Inc.) and 1% penicillin/streptomycin. They were incubated at 37°C in a humidified incubator gassed with 5% CO_2. Transfection was made at a confluence of ~80% by calcium phosphate precipitation. Enhanced green fluorescent protein was cotransfected as a surface marker. Experiments took place usually 10–28 h after transfection.

Single-channel recording

Single-channel currents were recorded using the outside-out configuration. The recordings were made mostly in oocytes, except for the double mutant (E636Q/D646N) and K639Q, which were recorded from HEK293 cells. The double mutant did not seem to express well in oocytes. Currents were amplified using an Axopatch 200B amplifier (MDS Analytical Technologies), low-pass filtered at 5–10 kHz through the built-in eight-pole Bessel filter, and sampled at 10–20 kHz with a multifunctional data acquisition card (National Instruments). Patch pipettes were fabricated from borosilicate glass capillary (Sutter Instrument Co.) and fire polished to a resistance between 5 and 10 MΩ when filled with 150 mM KCl solution. Pipette series resistance and capacitance were compensated using the built-in circuitry of the amplifier, and the liquid junction potential between the pipette and bath solutions was zeroed before seal formation. Currents were normally evoked from a holding potential of either −60 mV (inward) or +60 mV (outward). All voltages were defined as membrane potentials with respect to extracellular solutions.

The bath solutions for oocytes consisted of (in mM): 140 K-gluconate, 10 KCl, 5 EGTA, and 10 HEPES, pH 7.4 (adjusted with KOH). The solutions for HEK293 cells were similar, except that 150 KCl was used instead of K-gluconate. Agonists were delivered by local perfusion of patches with appropriate external solutions. The external and internal pipette solutions were always symmetrical (except for the addition of agonists), and unless indicated, they were also the same as the bath solutions. In a subset of experiments, the pipette solution was supplemented with FVPP, a mixture of phosphatase inhibitors containing (in mM): 5 KF, 0.1 K_3VO_4, and 20 $K_3HP_2O_7$ (Liu and Qin, 2005). The FVPP solution has effects on preventing channels from rundown due to loss of phosphatidylinositol 4,5-bisphosphate from membranes (Yao and Qin, 2009). The exchange of external solutions was performed using a gravity-driven perfusion system with manually controlled solenoid valves (ALA Scientific Instruments). Buffers used for low pH solutions were Mes for pH 3.5–6.5, HEPES for pH 7.0–7.4, and Tris for pH 8.5–9.0. Solutions were titrated to their nominal pH at room temperature (23°C). For recordings in HEK293 cells, 50 µM amiloride was included to block native ASIC channels. Capsaicin was purchased from Fluka. Capsazepine was from Precision Biochemicals. All other chemicals were from Sigma-Aldrich. Capsaicin and capsazepine were dissolved in 100% ethanol to make a 1-mM stock solution, stored at 4°C, and diluted into the recording solutions at appropriate concentrations before experiments (0.001–0.1% final ethanol). All perfusion apparatus were thoroughly washed using ethanol after experiments.

Data analysis and modeling

Several models were attempted to describe the effects of protons on the unitary current amplitudes of TRPV1 channels. The first was the Woodhull model, which assumes that protons bind to a site in the channel and completely block current flow on a rapid timescale (Woodhull, 1973). The apparent unitary current, i, is related to the maximum current in the absence of blockers, i_0, by

$$i / i_0 = \frac{1}{1+\left(\frac{[H^+]}{K_H}\right)^n}, \quad (1)$$

where K_H is the dissociation constant for proton binding and n is the Hill coefficient to account for cooperative binding on multiple subunits. For sites with an electrical distance δ from extracellular solutions, the dissociation constant K_H is related to the membrane potential, V, by

$$K_H = K_{H,0} e^{\frac{z\delta VF}{RT}}, \tag{2}$$

where z is the valence, $K_{H,0}$ is the dissociation constant at 0 mV, and RT/F = 25 mV. The model was fit to the unitary current amplitudes obtained at different membrane potentials and external pHs.

The second model incorporates competitive inhibition of protons with permeating ions (Brelidze and Magleby, 2004). Under the condition of symmetric inside and outside solutions, the unitary current i follows

$$i = \frac{i_{\max}}{1+\left(\frac{K_S}{[S]}\right)^n \cdot \left(1+\frac{[H^+]}{K_H}\right)^n}, \tag{3}$$

where K_S and K_H represent the apparent dissociation constants of permeating ions (S) and protons, respectively, n is the pseudo Hill coefficient, and i_{max} is the maximum current amplitude.

The last model assumes that protons exert a screening effect on the surface charges of membranes and channel vestibules. The Gouy-Chapman-Stern equation is used to relate the membrane surface potential, ψ_0, to the free surface charge density, σ:

$$\sigma^2 = 2\varepsilon\varepsilon_0 RT \sum_i c_i \left[\exp\left(-\frac{z_i \psi_0 F}{RT}\right) - 1\right], \tag{4}$$

where ε is the dielectric constant for aqueous solutions, ε_0 is the polarizability of free space, c_i is the concentration of the i-th ion in the bulk solution, z_i is the corresponding valence, and R, T, and F are standard constants. The screening of the surface charges by protons is modeled by simple one-to-one binding (Zhang and Siegelbaum, 1991). The free surface charge density σ at a given proton concentration is determined from the total surface charge density, σ_0, by

$$\sigma = \frac{\sigma_0}{1+\frac{[H]_m}{K_H}}, \tag{5}$$

where K_H is the apparent dissociation constant of proton binding and $[H]_m$ is the proton concentration at the membrane surface. $[H]_m$ is related to the proton concentration in the bulk solution, $[H]_0$, through the Boltzmann equation:

$$[H]_m = [H]_0 \exp\left(-\frac{\psi_0 F}{RT}\right), \tag{6}$$

where ψ_0 is the surface potential defined by Eq. 4. Similarly, the concentration of the permeating ion at the membrane surface follows

$$[S]_m = [S]_0 \exp\left(-\frac{\psi_0 F}{RT}\right), \tag{7}$$

where $[S]_0$ is the concentration of the ion in the bulk solution. The unitary current is represented in terms of the local ionic concentration by the Michaelis-Menten model:

$$i = \frac{i_{\max}}{1+\left(\frac{[S]_m}{K_S}\right)^n}, \tag{8}$$

where i_{max} is the maximum unitary current amplitude and K_S and n have the same definitions as in Eq. 3.

The fitting of the above models to the experimental data were performed in MATLAB (The MathWorks) using the standard least-squares optimizers. For the last model of surface charge screening, the free parameters were chosen to be the total charge density σ_0, the dissociation constants K_H and K_S, the Hill coefficient n, and the maximum current i_{max}. At each iteration of optimization, the Gouy-Chapman-Stern equation was solved for a given charge density σ_0 to obtain the surface potential ψ_0. With our solution compositions, the equation was dominated by the monovalent ions and consequently could be simplified into a quadratic equation in terms of $\exp(-\psi_0 F/RT)$, which could be solved analytically. The resultant surface potential ψ_0 was used to evaluate the concentrations of ions on the membrane surface and then the unitary current i according to Eq. 8.

RESULTS

Extracellular protons reduce unitary current amplitudes

To examine the inhibitory effects of protons on the conductance of TRPV1, we recorded single-channel currents from outside-out patches of oocyte membranes expressing the channels under various extracellular pH conditions. Currents were elicited by local perfusion of 1 μM capsaicin, and the extracellular pH was varied in a range from 4.0 to 9.0. Fig. 1 A illustrates representative recordings at a holding potential of either −60 or +60 mV. As pH was decreased, the amplitude of the single-channel current was profoundly reduced at both membrane potentials, and at pH 4, the current became close to the baseline noise. To quantify the changes, we constructed all-point histograms and measured the unitary current amplitudes by fitting the histograms with Gaussians. Fig. 1 B displays the histograms obtained at different pH values along with their best Gaussian fits. At 2 kHz low-pass filtering, the histograms were slightly skewed due to intermediate amplitudes resulting from low-pass filtering. However, the effects of filtering distortion appeared to be negligible because the histograms remained adequately fitted by Gaussians, as shown by the solid lines in Fig. 1 B. The channel also sometimes exhibited subconductance levels, but their occurrences were relatively infrequent, so we restricted our analysis to the dominant conductance levels. Fig. 1 C summarizes the unitary current amplitudes from the fitting as a function of extracellular pH. The effects of protons spanned the entire pH range from 4 to 9. At −60 mV and normal pH (7.4), the current amplitude was ∼4.5 ± 0.1 pA (n = 12). Lowering the pH to 5.5 reduced it to ∼1.6 ± 0.1 pA, corresponding to a 65% reduction. Increasing the pH to 8.5, on the other hand, increased the current amplitude to 5.8 ± 0.2 pA, giving a 28% increase. Similar changes were observed

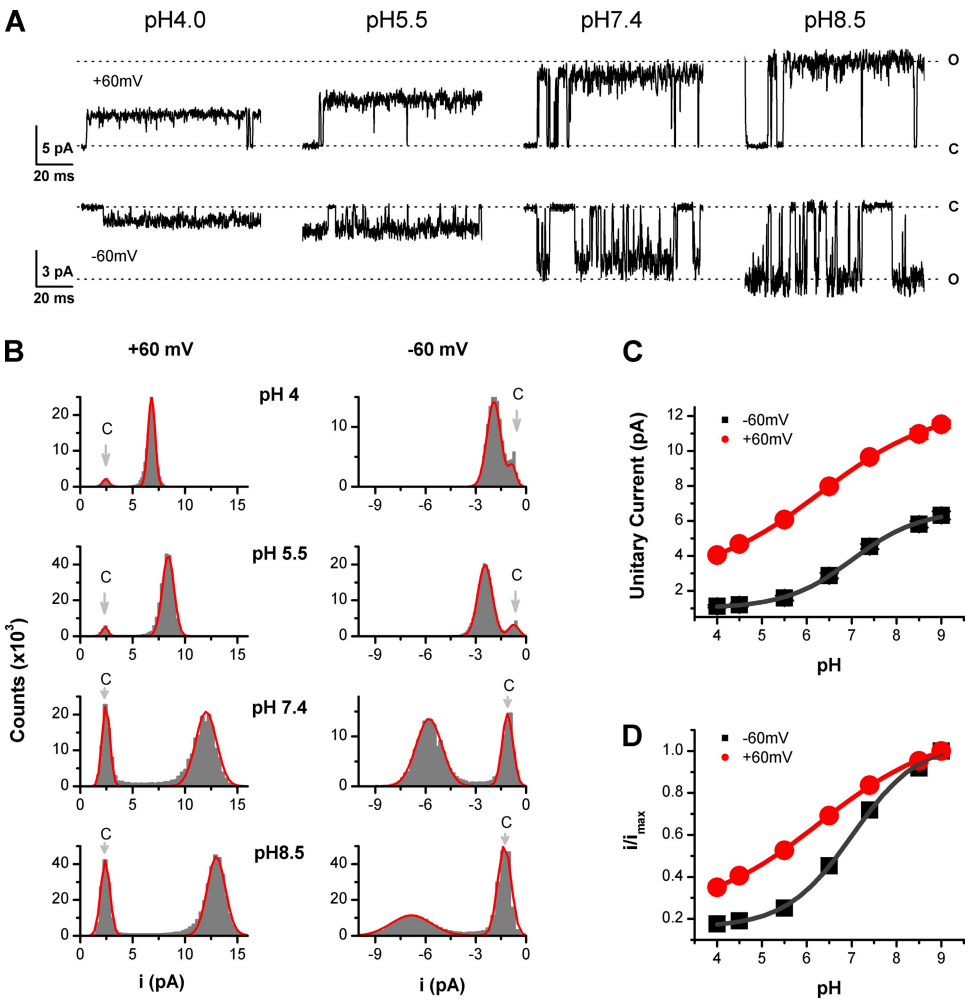

Figure 1. Extracellular protons reduce single-channel conductance of TRPV1 channels. (A) Representative single-channel currents at the indicated pH recorded from an outside-out patch of oocyte membrane expressing TRPV1. The external and internal solutions were symmetrical 150 mM KCl. Recordings at two membrane potentials were shown (±60 mV) and were low-pass filtered at 2 kHz. (B) All-point amplitude histograms of single-channel currents. The histograms were fit to sums of two Gaussian functions to determine the closed and open amplitudes. The solid lines represent best fits. (C) Dose–response curves for the unitary current amplitudes obtained at ±60 mV versus the extracellular pH. The solid lines represent fits to the Hill equation with pKa ~ 7, Hill coefficient of $n \sim 0.6$ for $V_h = -60$ mV, and pKa ~ 6 and $n \sim 0.3$ for $V_h = +60$ mV, respectively. (D) Normalized dose–response relationships showing different dependence on pH at different membrane potentials (±60 mV).

for the outward current at +60 mV. Acidifying pH from 7.4 to 4.5 reduced the current amplitude by 52%, whereas elevating pH to 8.5 resulted in an increase of 14%. The effects increased with proton concentrations in a dose-dependent manner. The solid lines in Fig. 1 C represent the fits to Hill's equations with $pK_a = 7$ and $n_H = 0.6$ for $V_h = -60$ mV and $pK_a = 6.3$ and $n_H = 0.3$ for $V_h = +60$ mV, respectively. These apparent pKa values were considerably higher than predicted by the free acidic amino acids in aqueous solutions. The fitting also showed that voltage affected the unitary current amplitudes and their pH dependences. Fig. 1 D replots the titration curves of the unitary current amplitudes after being normalized to their maximum values at pH 9. It is evident that the pH dependence became steeper at hyperpolarizing potentials, indicating increased cooperativity of proton binding at these potentials.

We note that the single-channel traces in Fig. 1 A were chosen to emphasize the current amplitude changes and may not faithfully reflect the kinetics of the channel. In general, the open probability of the channel became considerably higher at low pH and depolarizing voltages. This can be seen from the amplitude histograms in Fig. 1 B, where the open component became increasingly more dominant as the external pH was reduced. The increase of Po manifests with elongation of opening bursts and shortening of gaps that separate the bursts. At pH 5.5, the channel became almost constantly open at 1 µM capsaicin. Such a gating pattern is against protons as a slow pore blocker, which would result in more frequent occurrences of closures within the bursts. The opening of the channel was also associated with strong noise, which tended to be more profound at hyperpolarized potentials and appeared at all pHs. In some patches, the opening of the channel was sporadic and brief in durations at −60 mV, even with the application of 1 µM capsaicin, resulting in a spiky appearance. Adding FVPP, a mixture of phosphatase inhibitors, to the internal solution was able to alleviate the problem, suggesting that the channel may be in a "rundown" state in these patches due to loss of phosphatidylinositol 4,5-bisphosphate upon the excision of patches from cells (Yao and Qin, 2009).

Proton block is voltage dependent

The Woodhull model represents a common mechanism for voltage-dependent pore block of ion channels. To

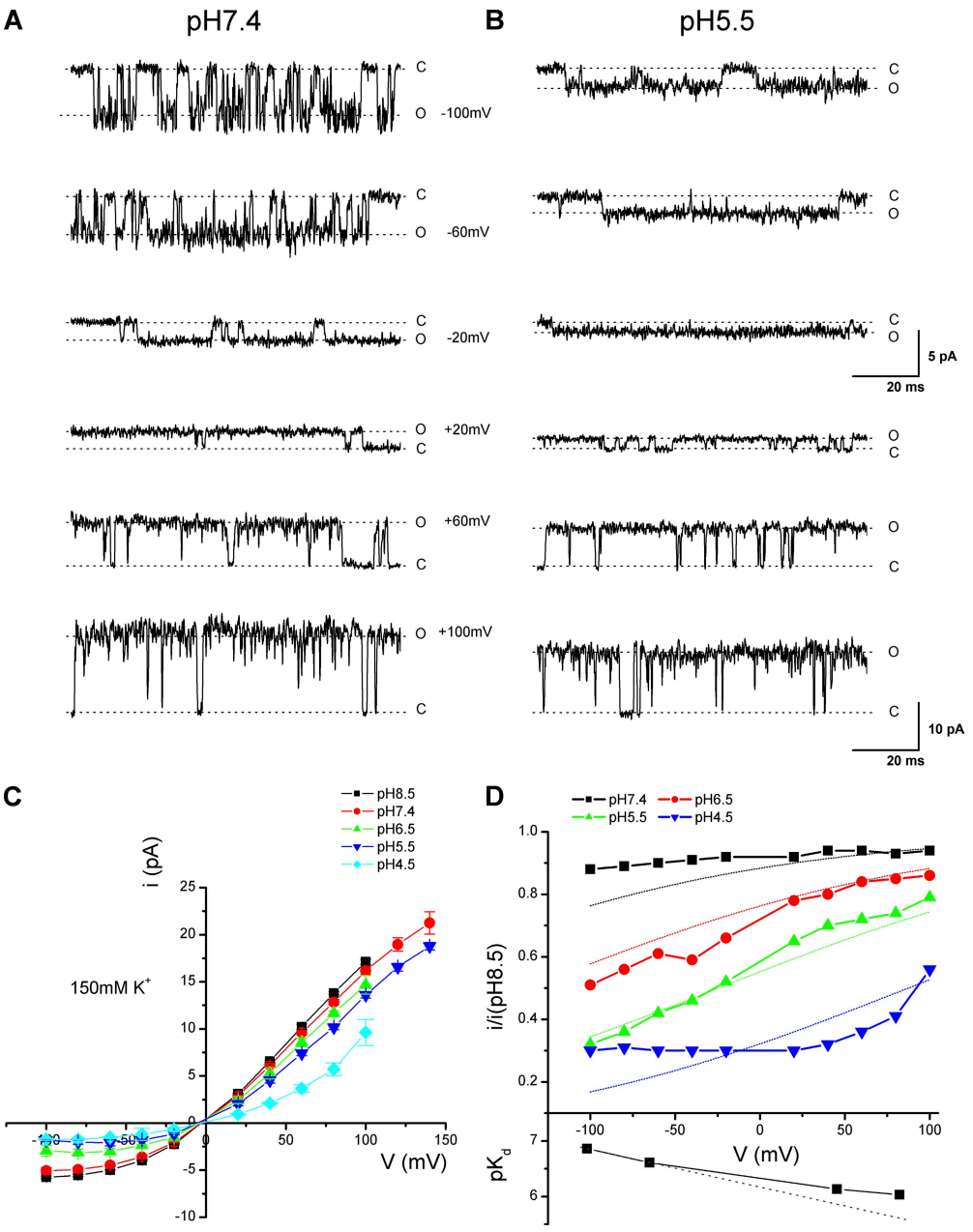

Figure 2. Voltage dependence of proton block of single-channel conductance. (A and B) Representative single-channel currents recorded at two extracellular pHs with different voltages ranging from −100 to +100 mV. (A) pH 7.4 and (B) pH 5.5, recorded with symmetrical 150-mM KCl solutions. (C) Single-channel i-V curves at different values of pH_os as indicated. The smooth lines were polynomial fits. (D; top plot) Ratio of the unitary current amplitudes at each pH_o (7.4, 6.5, 5.5, and 4.5) to the amplitudes at pH 8.5 plotted as a function of voltage. The dashed lines represent the best fit to a Woodhull model, which corresponds to an electrical distance d = 0.5 for the binding site from the bulk solution, an apparent valence z = 1, a dissociation constant $pK_{d,0}$ = 5.3 at 0 mV, and a pseudo Hill coefficient n = 0.4. The model was globally fit to the unitary current amplitudes at different pH values. (Bottom plot) pKd of proton inhibition estimated from the Hill equation fit at each voltage.

determine whether the proton block of TRPV1 follows such a mechanism, we examined its voltage dependence in more detail. Single-channel currents were recorded under various voltages and external pHs (Fig. 2, A and B). To simplify model calculations, the internal and the external solutions were kept symmetrical and contained 150 mM K^+. Fig. 2 C summarizes the voltage dependence of the unitary current amplitudes at each pH ranging from 4.5 to 8.5. The i-V relationships rectified at all pHs, showing a relatively linear increase at depolarizing potentials and a sublinear dependence at hyperpolarizing voltages. The rectification is not characteristic to the Goldman-Hodgkin-Katz–type current equation because the ionic conditions were symmetrical, suggesting that the permeability of the channel to ions were voltage dependent.

To evaluate the extent of proton block, we normalized the i-V curves at each pH to that of pH 8.5. As shown in Fig. 2 D, the normalized unitary current amplitudes remained relatively independent of voltage at pH 7.4, but they became voltage dependent at pH 6.5 and 5.5. At these pH values, proton block tended to be more significant at more negative holding potentials. The block also appeared to approach saturation at pH 4.5, where the currents were relatively unchanged over a broad range of hyperpolarizing potentials. Fig. 2 D also illustrates the pKd of the proton inhibition at different voltages, which appeared to depart from a linear voltage relationship and tended to increase at more negative potentials.

The voltage dependence of the proton effects suggests that protons enter the channel pore to a certain

distance and act on a site that lies within the transmembrane electrical field. To further quantify the voltage dependence, we fit the data with the Woodhull model (Eqs. 1 and 2). The dotted lines in Fig. 2 D represent simultaneous fits of the model to the normalized i-V relationships at all pH values (7.4–4.5). The fitting predicts an electrical distance of the binding site at $\delta = 0.5$ from the bulk solution, an apparent valence of $z = 1$, a dissociation constant of $pK_{d,0} = 5.3$, and a pseudo Hill coefficient of $n = 0.4$. The model explained the data reasonably well at pH 6.5–5.5, giving increasing blockade at hyperpolarizing voltages. However, it appeared to depart at more acidic pHs. At pH 4.5, the model predicted a persistent voltage dependence similar to that at higher pHs, whereas the data displayed a saturating behavior. In addition, the model implies that the unitary conductance should be diminished at sufficiently high blocker concentrations, but the actual measurements of the unitary currents at saturating pH remained significant. The Woodhull model assumes a static pore structure and no interactions between blockers and conducting ions, so that the apparent unitary current in the presence of blockers is proportional to the unblocked probability of the pore. The discrepancy of the fittings suggests that the inhibition of TRPV1 by protons involves a more complex mechanism.

Effects of surface charges

Protons may also reduce the single-channel conductance by neutralizing negative charges on the lipid head groups of membranes and/or in the vestibule region of channel pores. The neutralization of the negative charges will result in a reduction of the surface potential and consequently decreases the local concentration of ions near the channels. To examine the role of surface charges in proton inhibition of TRPV1 conductance, we varied K^+ concentrations from 25 to 2,000 mM. For simplifying modeling, we again maintained the solutions on the two sides of membranes to be symmetrical. Single-channel currents were recorded at each ionic concentration for three extracellular pHs (5.5, 7.4, and 8.5). Fig. 3 A illustrates examples of the recordings with $[K^+] = 1$ M at ±60 mV. It is notable that even at this relatively high ionic concentration, protons remained effective in inhibiting the unitary currents of the channel. Fig. 3 (B and C) summarizes the measured unitary current amplitudes plotted against ionic concentrations for each pH_o. At both holding potentials (±60 mV), the current amplitudes exhibited a dose-dependent increase with $[K^+]$ and approached saturation at $[K^+] \geq 1$ M. Importantly, the saturating current amplitudes appeared significantly different with different pH_os. Thus, increasing the ionic strength of solutions was unable to fully relieve proton block, although the degree of the inhibition was reduced (Fig. 3, F and G). This result is inconsistent with the surface charge screening theory, which predicts that the electrostatic effects of protons would be relinquished at sufficiently high ionic concentrations. The dotted lines in Fig. 3 (B and C) show the best fits of the data to the Gouy-Chapman-Stern model (Eqs. 4–8; data at ±60 mV were fit separately). As expected, the model gave rise to a convergent maximum unitary current amplitude at high $[K^+]$ for different pH_os.

The effectiveness of protons at saturating ionic concentrations also argues against another common pore block mechanism, i.e., the competitive inhibition by which protons bind to the same sites as the conducting ions to block ion flows. Similar to surface charge screening, the model predicts that at a given pH_o, increasing $[K^+]$ would eventually diminish the effects of protons because they act competitively. Fig. 3 (D and E) shows the theoretical fits (dotted lines) to the model (Eq. 3; data at ±60 mV fit separately). Although the model showed a dose-dependent increase of the unitary current amplitude with $[K^+]$, it failed to reproduce the saturation behaviors at different pH_os. The models tended to underestimate the extent of inhibition by protons at saturating $[K^+]$ while overestimating the effects at submaximal ionic concentrations.

Neutralization of D646 partially relieves pH dependency of block

The models we have examined assume a static pore and protons exert their effects by either reducing local ionic concentrations or blocking ion flows through the pore. The inability of these models to describe the data suggests that the blockade by protons of TRPV1 may instead involve dynamic changes in the pore structures. To test this hypothesis, we resorted to mutagenesis to identify the molecular basis of proton inhibition. The pore region of TRPV1 is homologous to that of KcsA. By sequence alignment, we could locate the putative selectivity filter (TIGMG, conserved among TRPV channels) and then delineate the vestibular region and the pore helix that flank the filter. We first examined the negatively charged residues in the vestibular region at the pore entrance. The residues were each neutralized, and their effects on the reduction of unitary currents by protons were evaluated. Among them, D646 was found to be most effective. Fig. 4 A illustrates the single-channel currents recorded from the mutant at 1 M K^+. The reduction of the unitary current amplitudes from pHs 8.5 and 5.5 was noticeably less significant than the wild type, especially at the depolarizing voltages (+60 mV). Fig. 4 (B and C) summarizes the unitary current amplitudes versus the ionic concentrations at three pHs (5.5, 7.4, and 8.5) and the two tested membrane potentials. At pH 5.5, the dose–response curves of the mutant appeared similar to those of the wild type. But at pHs 7.4 and 8.5, the maximum currents became considerably reduced. The inhibition of the maximum currents was ~29% at −60 mV and ~13% at +60 mV, respectively,

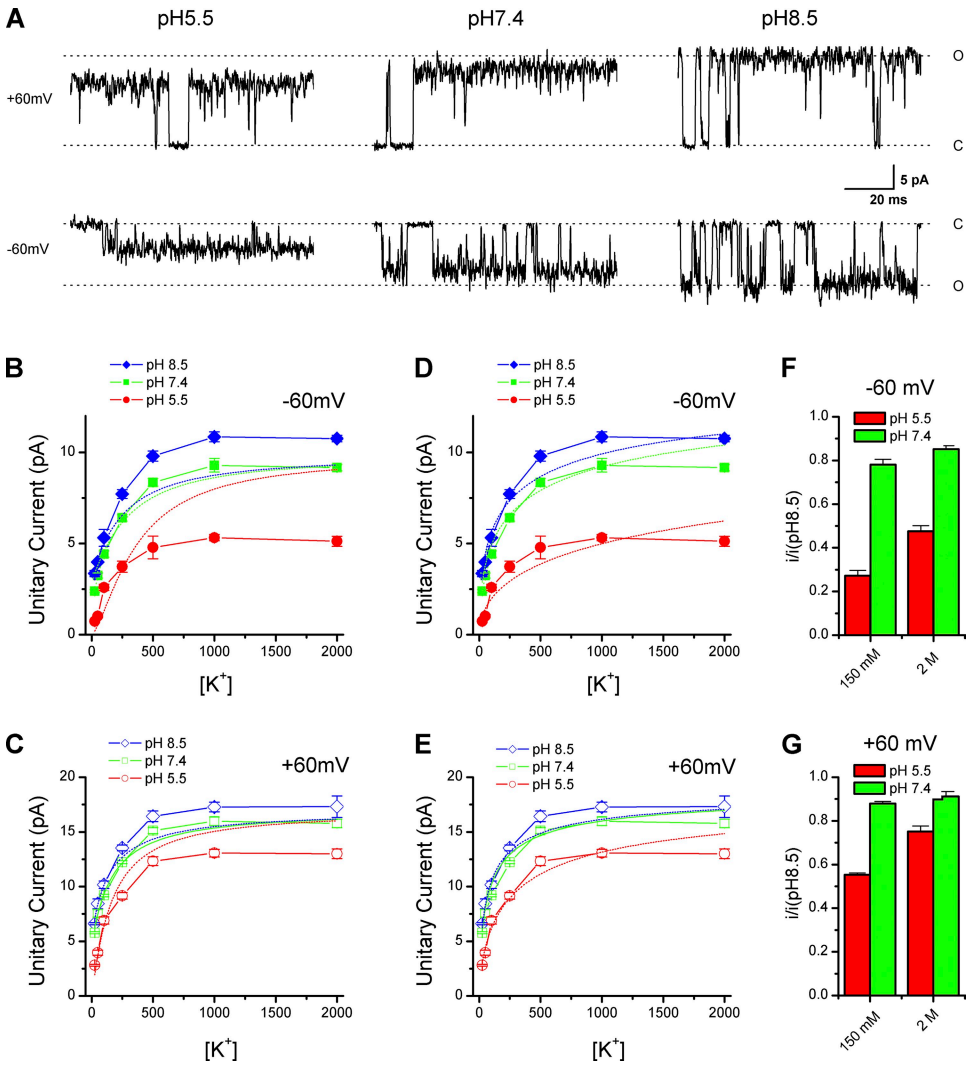

Figure 3. Effects of ionic strength on proton block of TRPV1 channels. (A) Representative single-channel currents from TRPV1 channels recorded in symmetrical 1,000-mM KCl solutions at different voltages and extracellular pHs as indicated above traces. (B and C) Dose-dependent relationships of the unitary current amplitudes versus $[K^+]$ at −60 mV (B) and +60 mV (C), respectively. Note that the dose–response curves were saturated at different maximal current amplitudes with different pHs. Dashed lines represent predictions of the Gouy-Chapman-Stern model based on simultaneous fitting of the data at multiple extracellular pHs. The model assumes that protons exert their effects by one-to-one binding to negative surface charges on the membrane to lower local H^+ and K^+ concentrations. At high $[K^+]$, it predicted a common maximal current amplitude independent of extracellular pH. The fits correspond to the following parameter values: σ = 0.2e/nm^2, pKa = 7 for protonation of surface charges, K_S = 372 mM for the dissociation constant of K^+ ion binding, n = 1.5 for the apparent Hill coefficient, and i_{max} = 10 pA for the maximum current amplitude (−60 mV); σ = 0.1e/nm^2, pKa = 7.2, K_S = 160 mM, n = 1.1, and i_{max} = 17 (+60 mV). The surface potentials Ψ_0 at 2 M K^+ for pHs 8.5, 7.4, and 5.5 were, respectively (in mV): −18, −15, and −0.6 (−60 mV), and −17, −12, and −0.4 (+60 mV). (D and E) Fits to a competitive inhibition model in which protons bind to the same sites occupied by K^+ to block ion flows. Data at different pHs were fit simultaneously. The fit yields the following model parameters: K_S = 219 mM for the dissociation constant of K^+ binding, pK_a = 6.5 for proton binding, n = 0.5 for the pseudo Hill coefficient, and i_{max} = 15pA (Vh = −60 mV); Ks = 70 mM, pKa = 5.8, n = 0.7, and i_{max} = 19 pA (Vh = +60 mV). (F and G) Effects of $[K^+]$ on proton inhibition at the indicated membrane potentials. The ratios of the unitary current amplitudes at pHs 7.4 and 5.5 to the amplitudes at pH 8.5 were plotted.

when pH_o was decreased from 8.5 to 5.5. For comparison, the wild type exhibited an inhibition of ∼51% at −60 mV and 24% at +60 mV. Thus, neutralization of D646 resulted in a >50% reduction in proton inhibition. Nevertheless, the mutant remained inhibited by low pH albeit to a less extent, and the inhibition was more profound at hyperpolarizing potentials, suggesting that the voltage sensitivity of the blockade was remained. Also like the wild type, the mutant channel had dose–response curves saturating at different maximum current amplitudes with different pH_os. Collectively, these data indicate that D646 is important but partially responsible for proton block of the channel conductance.

It is noteworthy that the D646N mutation reduced the proton block of the unitary conductance by suppressing the maximum current amplitudes at high pH without significantly altering the amplitudes at low pH. This is parallel to the phenotype of the wile type at low pH, suggesting that the residue could be directly protonated. In addition, the maximum currents at saturating $[K^+]$ differ from those of the wild type at both pH 7.4 and 8.5, indicating that the residue did not play a simple electrostatic effect to perturb local ionic concentrations; otherwise, the neutralization effects of the residue on the unitary currents would diminish at high $[K^+]$.

E636 also contributes to proton block

To identify additional residues for proton inhibition, we extended our search to residues in other regions of the pore loop. Besides those on the pore entrance, TRPV1

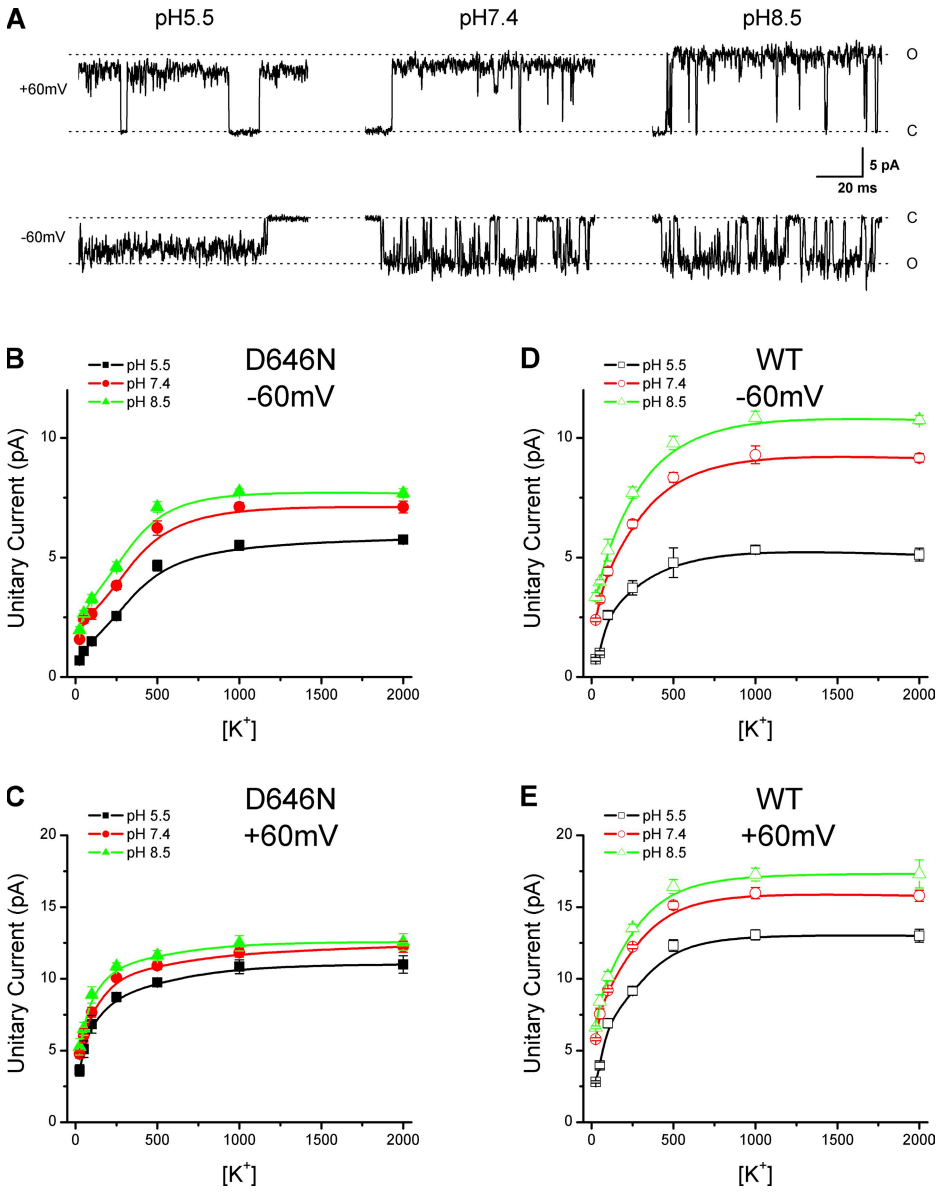

Figure 4. Neutralization of D646 partially relieves proton block. (A) Representative single-channel current traces from the D646N mutant at different extracellular pHs. (Top row) Outward currents at +60 mV. (Bottom row) Inward currents at −60 mV. Solutions were symmetrical and contained 1 M KCl. (B–E) Plots of unitary current amplitudes versus ionic concentrations for the mutant channel at the indicated pH_o (B, −60 mV; C, +60 mV). For comparison, similar plots for wild type are displayed in D and E.

contains a glutamic acid, E636, on the putative pore helix. The residue was located at a position approximately two helical turns from the bottom of the selectivity filter. We neutralized the residue by substitution with glutamine and measured the sensitivity of the unitary current amplitudes to extracellular pH. Fig. 5 A shows single-channel currents recorded from the mutant at different pHs in symmetrical $[K^+]$ = 1 M. Similar to D646N, the E636Q mutant remained sensitive to protons, but the extent of inhibition was considerably less than the wild type. Fig. 5 (B and C) plots the resultant unitary current amplitudes versus $[K^+]$ at pHs 5.5, 7.4, and 8.5, respectively (B, −60 mV; C, +60 mV). Compared with those of the wild type, the maximum currents of the mutant were similar at low pH but became suppressed at high pHs (Table I). Protons became less effective in inhibiting the unitary currents of the mutant channel. The mutation caused the channel to more resemble the wild type at low pH. These changes were parallel to those of the D646N mutation, suggesting that the two residues may exert their functions through similar mechanisms. In addition, the unitary currents of the E636Q mutant exhibited saturation at $[K^+] \geq 1$ M, and the corresponding maximum amplitudes remained different at different pH_os (Fig. 5, B and C, and Table I). These characteristics were also consistent with those of the wilt type and the D646N mutant, suggesting that the ionic concentration dependence of the currents had not been grossly altered by the mutation. The residual sensitivity of the maximum conductance to low pH lends further support that the inhibition of the unitary currents by protons involves mechanisms more than surface charge screening or pore blockade by occlusion of permeating ions.

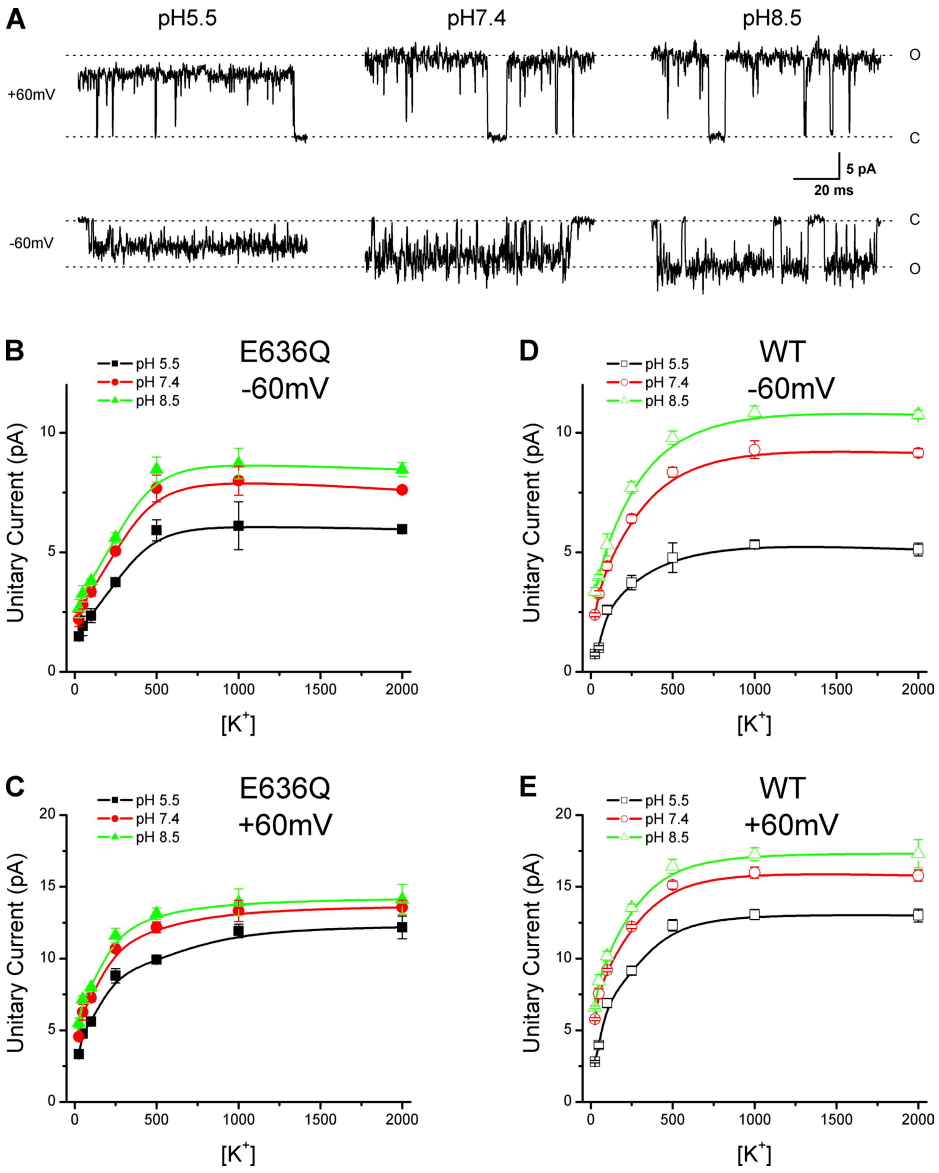

Figure 5. Neutralization of E636 reduces proton inhibition. (A) Representative single-channel currents from the E636Q mutant channel at different external pHs in symmetrical 1-M KCl solutions. Holding potential was either +60 mV (top row) or −60 mV (bottom row). (B and C) Plots of unitary current amplitudes versus $[K^+]$ at the indicated pHo. (B) V_h = −60 mV. (C) V_h = +60 mV. (D and E) Similar plots for wild type were shown for comparison.

The residue E636 was previously implicated in capsaicin activation of TRPV1 (Welch et al., 2000). Aside from unitary current amplitudes, we also noticed significant changes caused by the mutation E636Q in channel gating. At −60 mV, the wild type tended to open in relatively short bursts separated by long gaps of closures at normal or high pHs. Such long closures occurred much less frequently in the E636Q mutant, yielding a higher open probability. The neutralization of E636 rendered the channel to be more sensitive to agonists. These changes are also consistent with the effects of protons on the gating of the wild-type TRPV1, suggesting that the proton block of the unitary currents and the potentiation of gating may be mechanistically correlated.

TABLE I

Comparison of unitary current amplitudes for wild-type and mutant channels at $[K^+]$ = 1 M (current represented in pA as means ± SEM with n = 3–9)

	−60 mV			+60 mV		
	pH 5.5	pH 7.4	pH 8.5	pH 5.5	pH 7.4	pH 8.5
Wild-type	5.3 ± 0.2	9.3 ± 0.4	11 ± 0.3	13 ± 0.4	16 ± 0.4	17 ± 0.5
E636Q	6 ± 1	8 ± 0.6	8.7 ± 0.6	12 ± 0.5	13 ± 0.7	14 ± 0.9
D646N	5.5 ± 0.2	7 ± 0.2	7.8 ± 0.1	11 ± 0.5	12 ± 0.3	13 ± 0.5
E636Q/D646N	5 ± 0.1	5.4 ± 0.2	5.7 ± 0.2	8.2 ± 0.2	8.9 ± 0.2	9.3 ± 0.4

Double mutations D646N/E636Q abrogate proton block

Because both D646 and E636 were only partially effective, we examined the double mutant containing neutralization of both residues (D636N/E636Q). Fig. 6 (A and B) illustrates the single-channel currents from the mutant (A, +60 mV; B, −60 mV). Recordings at different pH_os (5.5–8.5) and ionic concentrations (25–2,000 mM) were displayed. For each $[K^+]$, the current amplitudes were similar when the external pH was varied from 8.5 to 5.5. Fig. 6 (C and D) further quantifies the unitary current amplitudes versus $[K^+]$ at different $[H^+]_o$s (C, −60 mV; D, +60 mV). The currents of the double mutant (Fig. 6, C and D, solid lines) were nearly invariable to perturbation of extracellular pH. Furthermore, at −60 mV, the dose–response curves of the currents versus $[K^+]$ were nearly overlapping with that of the wild type at pH 5.5 (Fig. 6 C, dotted line, black). At +60 mV, the wild-type currents at pH 5.5 remained considerably larger than the mutant (Fig. 6 D). This difference appeared to arise because of a lower pK_a at the depolarization voltages. When the extracellular pH was decreased to 4.5, the unitary currents of the wild type were further reduced and became similar to those of the mutant (Fig. 6 D). The double-mutant channel thus fully mimicked the wild type at saturating low pHs, indicating that the protonation of the D646 and E636 residues was able to adequately account for the inhibition of the unitary conductance in wild-type channels. It is also noteworthy that the outward currents of the double mutant remained significantly larger than the inward currents (e.g., 5.4 ± 0.2 pA at −60 mV vs. 8.9 ± 0.2 at +60 mV for pH 7.4 and $[K^+]$ = 1 M; n = 7), which suggest that D646 and E636 were not responsible for the voltage dependence of the conductance of the channel.

Proton block is local to the pore region

Given that the residues for proton block, especially E636, also affect the kinetics of channel gating, we asked whether the proton block of the conductance involves global conformational changes or is a local property of

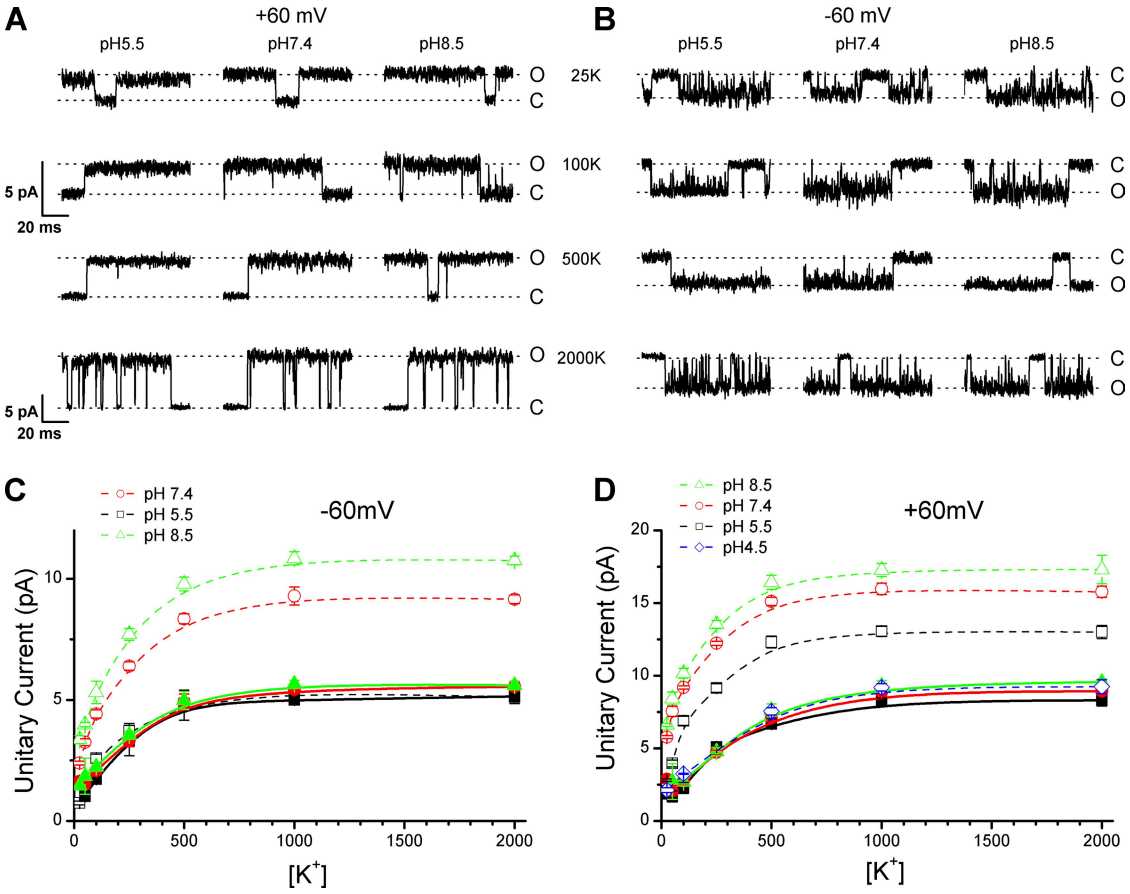

Figure 6. Double mutations of D646 and E636 abrogate proton block. (A and B) Examples of single-channel currents from the double mutant D646N/E636Q, showing little changes in the unitary current amplitudes with changes in extracellular pH at several ionic concentrations ($[K^+]$ = 25, 100, 500, and 1,000 mM). (A) Holding potential of +60 mV. (B) Holding potential of −60 mV. Solutions were symmetrical on both sides of membranes. (C and D) Plots of unitary current amplitudes versus $[K^+]$ at the indicated pH. (C) −60 mV. (D) +60 mV. Solid lines indicate double mutant, and dashed lines are for wild type. The unitary current amplitudes of the double mutant were similar to those of wild type at low pH and were independent of extracellular pH changes over a broad range of ionic concentrations (25–2,000 mM). The mutant did not show a detectable expression in oocytes. All recordings were from HEK293 cells.

the pore region. To address this issue, we examined the mutant channel V538L. The V538L mutation was able to selectively abrogate proton activation of TRPV1 while retaining normal responses to other stimuli, including capsaicin and heat (Ryu et al., 2007). If the effects of protons on the unitary conductance and the channel activation are tightly coupled, we might expect that the mutation would also affect the inhibition of the single-channel current amplitudes by low pH. Fig. 7 A shows the single-channel recordings from the mutant evoked by capsaicin at different extracellular pHs with symmetrical 2 M K^+. It is evident that the conductance of the mutant remained sensitive to pH_o. Fig. 7 (C and D) compares the average unitary current amplitudes of the mutant with those of the wild type. The two were similar over all tested pHs (8.5–5.5). Thus, the V538L mutation, although abrogating proton activation, did not alter the effects of protons on the channel conductance.

We also tested another mutant, E600Q. The residue E600 is required for proton potentiation of TRPV1 (Jordt et al., 2000). Neutralization of the residue eliminates the sensitization of capsaicin and heat responses by low pH. As shown in Fig. 7 B, the E600Q mutant was also inhibited by protons at both ±60 mV. At V_h = +60 mV, the mutant appeared to show a slightly reduced unitary current amplitude. The difference, however, was relatively small (<10% at +60 mV and 2% at −60 mV). Furthermore, the inhibition of the unitary currents by protons remained profound, especially for the inward currents at −60 mV (Fig. 7 C). These results, together with those on V538L, suggest that the conductance effect of protons is mainly mediated by residues within the pore region and separate from the gating and activation by agonists.

DISCUSSION

We have investigated the effects of protons on single-channel current amplitudes of TRPV1. Our results confirmed previous reports that protons reduce the unitary conductance of the channel (Baumann and Martenson, 2000; Ryu et al., 2003). To address the mechanisms, we measured the dependences of the unitary current amplitudes on voltage, extracellular pH, and ionic concentrations. All experiments were performed with single-channel recording to more precisely isolate the conductance effects. We showed that protons reduced the unitary currents in a dose- and voltage-dependent manner, similar to proton blocks observed in other channels and suggesting that protons bind to a site within the channel. The ionic concentration dependence, however, revealed that the maximum conductance

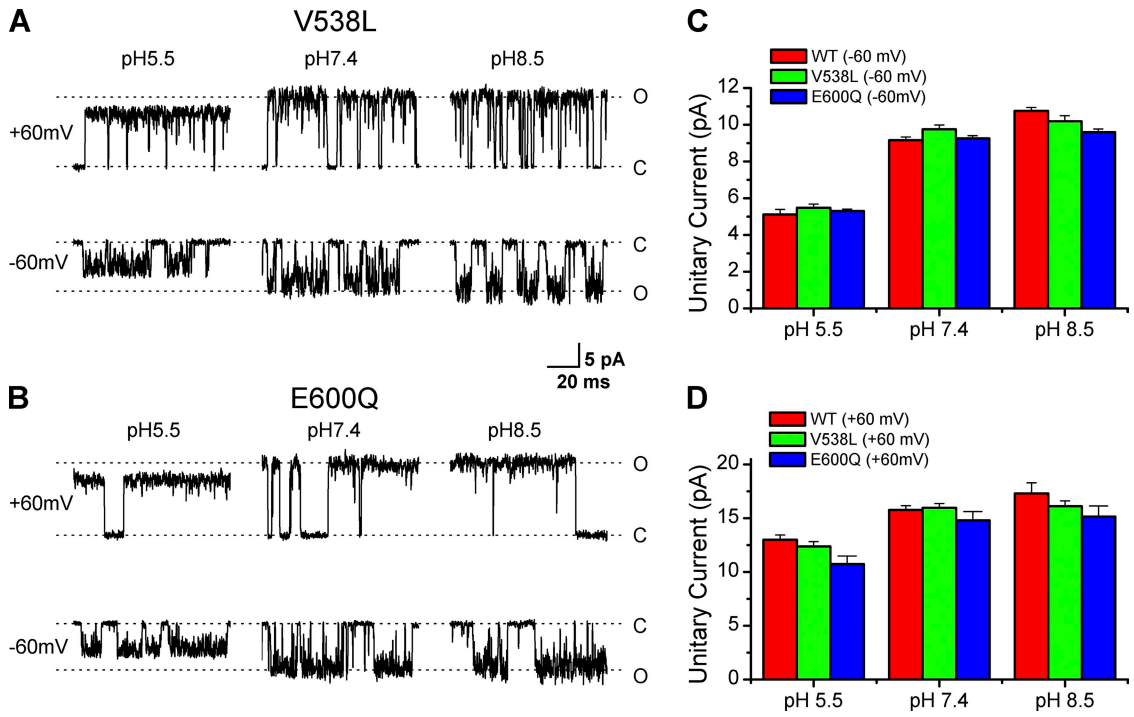

Figure 7. Proton gating is not involved. (A) Representative single-channel currents from the mutant V538L channels at different extracellular pHs. Currents were evoked by 1 μM capsaicin at either −60 mV (bottom row) or +60 mV (top row) in symmetrical solutions (2 M KCl). The V538L mutation, which abrogates proton activation of TRPV1, did not eliminate proton inhibition of single-channel conductance. (B) Similar recordings from the E600Q mutant channels. Proton block of unitary current amplitudes remained after neutralization of E600, which abolishes the potentiation effect of low pH on channel activation and gating. (C and D) Comparison of unitary current amplitudes of the mutant channels with wild type at different pH values. (C) V_h = −60 mV. (D) V_h = +60 mV. Both mutants and the wild type had similar current amplitudes at each tested pH_o.

did not converge with different extracellular pH. Such a result was not expected with the conventional pore blockade mechanisms, such as the Woodhull model, the competitive inhibition mechanism (protons may or may not permeate through the pore), the surface potential theory, or their combinations. Mutagenesis experiments unraveled two acidic residues essential for the proton effects, one at the pore entrance and the other on the putative pore helix at the back of the selectivity filter (Fig. 8). Neutralization of these residues rendered the unitary current amplitudes to be no longer sensitive to external pH. The inhibition by protons is thus mediated by residues both on the permeation pathway and deep in the core of the pore.

Both the failure of the standard pore blockade models and the involvement of residues in the core of the protein suggest that the proton block of TRPV1 may involve changes in the pore structures. Two possible mechanisms may be hypothesized. One is that the pore region may adopt multiple conformations depending on extracellular pH. Binding of protons favors a conformation of lower conductance. Alternatively, the pore may not be static but rapidly fluctuating. Proton binding alters the rates of the fluctuation, which may result in changes in ion permeation. This is essentially a fast-block mechanism, except that the titration sites of protons involve residues that do not lie directly on the ion permeation pathway. Although both models may explain our data, they can be difficult to distinguish in practice. In theory, the first model would predict multiple pH-dependent discrete amplitudes. But the presence of multiple proton bindings among subunits may lead to a large set of possible combinations, which cause the amplitudes to vary seemingly continuously with pH. The second model predicts an increase in the noise when the channel is open. We noticed that the background open noise of TRPV1 is already high over the entire pH range. The double mutant, despite the insensitivity of its conductance to protons, also exhibited significant open-channel noise, suggesting that there are other more dominant noise sources, which make it difficult to isolate the pH-dependent components. The two models would give rise to effectively similar observations.

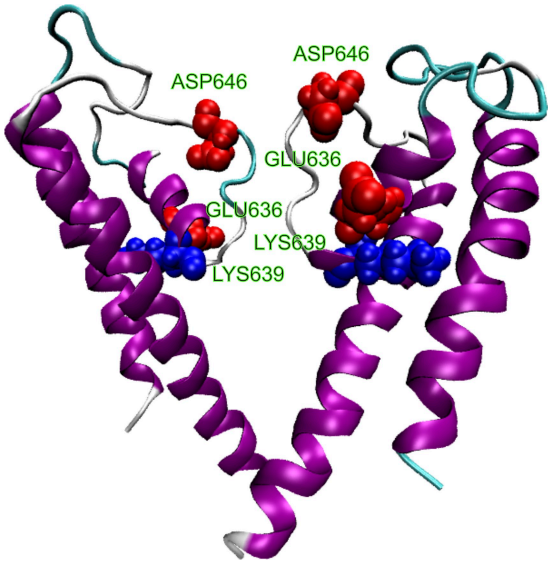

Figure 8. A homology model for the pore region of TRPV1 depicting the positions of the residues important for proton block (Glu636 and Asp646). Residue Glu636 is located on the pore helix, and Asp646 is immediately above the selectivity filter (TIGMG). Approximately one helical turn below Glu636 is another charged residue Lys639 (shown in blue). The model was constructed by homology modeling using the crystal structure of the KcsA channel as a template. See Ryu et al. (2007) for the alignment of sequences between the two channels.

The pore region of TRPV1 appears to be homologous to KcsA (García-Martínez et al., 2000; Welch et al., 2000; Rosenbaum et al., 2002; Ryu et al., 2007). Consistent with our hypotheses, there is good evidence that a KcsA-type pore may allow for a certain amount of conformational flexibility. Molecular dynamic simulations show a significant degree of flexibility and/or distortion in the filter region in KcsA or KcsA-based homologous models (Bernèche and Roux, 2000; Capener et al., 2003; Domene et al., 2004). The fluctuations of structures occur on a timescale comparable to mean passage times of K^+ ions through channels (~10 ns). Crystal structures of KcsA show differences between the low [K^+] and high [K^+] (Zhou et al., 2001), and at intermediate concentrations of cations, the electron density of the filter becomes distorted (Zhou and MacKinnon, 2003), implying multiple conformations of this region within the same crystal. In Kir 6.2 channels, nonpolar residues outside the selectivity filter are found to influence single-channel conductance without altering the relative permeability to intracellular Na^+ (Proks et al., 2001). Interestingly, one such residue, V127, is located at a position similar to E636 in TRPV1. Another inward rectifier channel, Kir2.1, exhibits single-channel kinetics with brief closures arising from the trapping of permeating ions in the selectivity filter, supporting coupling between ion conduction and gating (Lu et al., 2001). The voltage-dependent gating of KcsA channels requires charged residues on the pore helix, implicating possible rearrangement of the pore helix during channel activation (Cordero-Morales et al., 2006). The C-type inactivation of Kv channels is accompanied with transient increases in the permeability to smaller Na^+ ions, supporting possible constriction of the selectivity filter (Liu et al., 1996; Starkus et al., 1997; Zheng and Sigworth, 1997; Kiss et al., 1999; Bichet et al., 2003). Many K^+ channels also show a "defunct" state upon depletion of K^+ ions, whose formation involves deformation of the selectivity filter and dilation of pores (Loboda et al., 2001). In TRPV1 itself, it has been recently reported that the pore properties such as ionic selectivity and Ca^{2+} permeability

undergo time- and agonist concentration–dependent changes during channel activation, which also imply possible alterations of the selectivity filter (Chung et al., 2008).

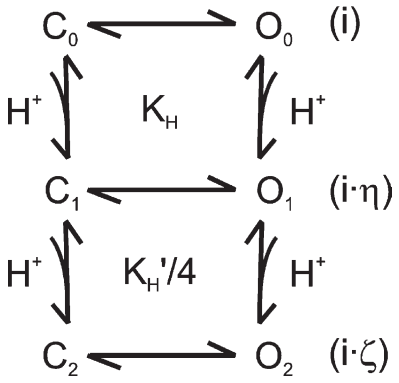

(SCHEME 1)

The dose–response curves of the blockage of TRPV1 by protons were relatively flat (Fig. 1) and had Hill coefficients below unity, in spite of a total of eight possible protonation sites. Such a weak concentration dependence has several implications: (1) the binding of protons to different sites is negatively cooperative, (2) the conductance is partially inhibited, and (3) the extent of inhibition increased with the level of proton binding. To elucidate the notions, we can consider a prototype inhibition model as illustrated in Scheme 1. The model involves two protonation sites and assumes that protons may bind to both closed and open channels, and that the binding and unbinding of protons occur on a fast timescale as compared with the gating of the channel (i.e., fast block). For such a scheme, it is possible to show that the concentration–response relationship of the apparent unitary currents will have a Hill coefficient below unity if, and only if,

$$\frac{K_H^{'}}{K_H} < \frac{4(\eta-\zeta)(1-\eta)}{(1-\zeta)^2}, \tag{9}$$

where K_H and K_H' are the association constants of proton binding to the first and the second site, respectively, and η and ζ represent the corresponding changes of the unitary current amplitudes relative to the full amplitude of the unprotonated channel. In a special case of $\eta = 1/2$ and $\zeta = 1/4$, for example, the condition becomes $K_H' < 8/9\ K_H$. That is, the binding of protons to the two sites is negatively cooperative. Eq. 9 also implies that the negative cooperativity of binding alone is insufficient to ensure the Hill coefficient to be <1, which is consistent with the modeling results on the gating cooperativity of voltage activation (Yifrach, 2004). The presence of partial conductance is required to further enhance the abundance of the intermediates. The inhibition of TRPV1 by protons is certainly more complex than Scheme 1. Nevertheless, the example demonstrates the possibility for a concentration–response curve to have a Hill coefficient <1 in the presence of multiple binding sites. In TRPV1, the negative cooperativity of proton binding may arise from the close proximity of the binding sites, where the protonation of one site may influence the binding of protons to the adjacent sites. Alternatively, it may also occur as a result of incremental changes of local structures after successive protonations. The implication of a partial inhibition of the conductance is in agreement with the observations that the channel retained measurable unitary current amplitudes at low pH.

The two acidic residues for proton inhibition of TRPV1 are located at positions similar to Glu71 and Asp80 in KcsA (Fig. 8). Many studies have been performed on the ionic state of these residues in KcsA channels. It appears to be a consensus that the two residues form a carboxyl–carboxylate interaction and share a proton between the two carboxylate at neutral pH (Ranatunga et al., 2001; Zhou et al., 2001; Bernèche and Roux, 2002; Bucher et al., 2007). In addition to the two acidic residues, the pore helix of TRPV1 contains another basic residue, Lys639, which is located about one helical turn below Glu636 and thus further into the core of the pore and more adjacent to the selectivity filter (Fig. 8). Both the low dielectric environment and the close proximity favor its interactions with Glu636 and Asp646. García-Martínez et al. (2000) previously showed that Lys639 and Glu636 can be swapped without compromising channel functions, and thus concluded that the two residues form a salt bridge. We noticed that Glu636 alone could also be neutralized, suggesting that Lys639 may also interact with Asp646, the only remaining acidic residue in its vicinity. Furthermore, the channel remained functional even after neutralization of both acidic residues, indicating that the side chain of Lys639 may be stabilized in the absence of salt bridges, presumably by forming strong hydrogen bonds with Gln636 and Asn646 in the double mutant. The presence of a basic residue close to the di-acid pair is expected to influence the pKa of the side chains of the acidic residues. Indeed, our experiments with the K639Q mutant showed that the residue could have an effect of regulating the channel conductance (Fig. 9). The removal of the positive charge at the position caused a reduction of unitary current amplitudes (Fig. 9 A) and an increase in proton inhibition (Fig. 9 B). In theory, the triad Glu636, Asp646, and Lys639 could form a rich network of hydrogen bonds and electrostatic interactions. Explicit modeling would be necessary to determine their protonation states, the nature of the interactions, and their influences on the conformations of the local structures of the pore.

Protons also activate TRPV1. The activation appears to involve global conformational changes, which span

at least the S3-S4 linker and the pore helix (Ryu et al., 2007). To address the extent of structural changes associated with the conductance effects of protons, we examined the mutant V538L. The mutation V538L on the S3-S4 linker selectively abolishes proton activation without affecting responses to capsaicin or potentiation by low pH. Our data showed that the mutant had similar unitary current amplitudes and pH dependences as the wild type, suggesting that the inhibition of conductance by protons is independent of proton-evoked activation of the channel. The other mutation, E600A, which eliminates the potentiation effects of protons on capsaicin and heat responses (Jordt et al., 2000), appears to also have little influence on the reduction of the unitary conductance by low pH. Compared with a nearly complete removal of the proton block of unitary current amplitudes by mutations D636Q and E646N, the results suggest that the conductance effects of protons are localized to the pore region and thus may be common to the currents evoked by all stimuli. Such local structural changes are also consistent with the fast-blocking kinetics of protons, which apparently occur on a timescale beyond instrument resolutions.

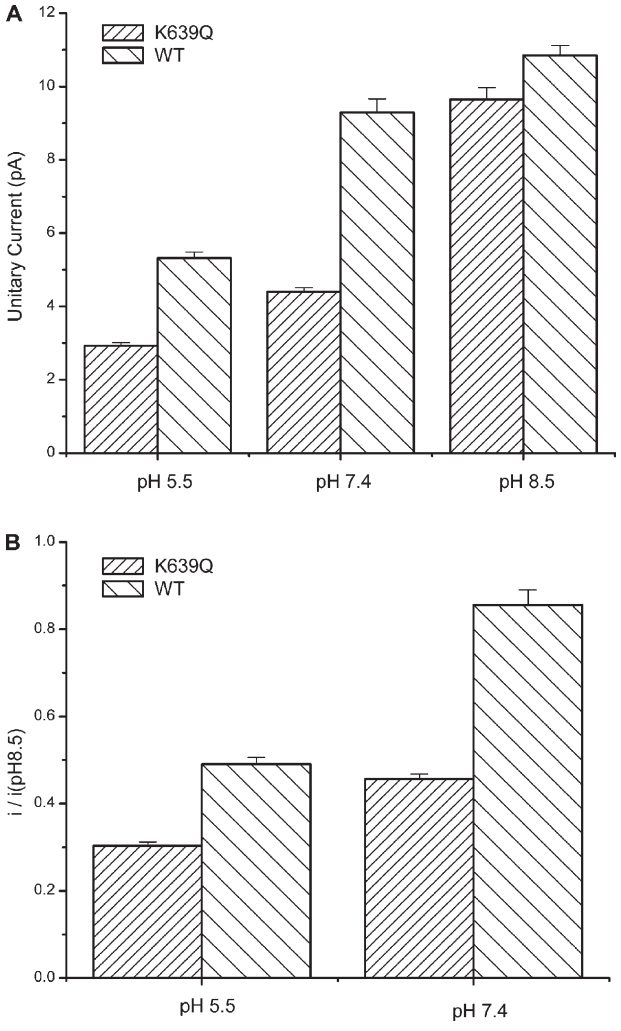

Figure 9. K639 modulates channel conductance and proton inhibition. (A) Unitary current amplitudes of the K639Q mutant versus the wild-type channel at different pHs. The removal of the positive charge caused a reduction of the current amplitudes at all pHs. (B) Ratio of the unitary current amplitudes at each pH to the amplitudes at pH 8.5, showing an increase in the inhibition by protons after charge removal. Single-channel currents were recorded from transiently transfected HEK293 cells in the outside-out configuration. $[K^+]$ = 1 M, V_h = −60 mV, and data points are means ± SE ($n \geq 5$).

Several residues in the pore region of TRPV1, including D646 and E636, have been previously studied for various functions. For instance, the residue Asp646 is shown to determine the binding of ruthenium red (García-Martínez et al., 2000). Asp646, Glu648, and Glu651 together influence the effects of protons on Ca^{2+} permeability (Samways et al., 2008). In our recordings, we have only seen a significant effect for Asp646 on proton block, and the difference may reflect the uses of different assays (single-channel recordings vs. whole cell and Ca^{2+} fluorescence measurements) and different permeating ions (monovalent vs. divalent). In addition, Asp646, Glu648, and Glu636 are demonstrated to selectively contribute to capsaicin gating (Welch et al., 2000), whereas Glu648 and Glu600 are implicated in proton potentiation and activation (Jordt et al., 2000), and cation modulation of agonist sensitivity (Ahern et al., 2005; Ohta et al., 2008). More recently, Asp646 and Asp648 are shown to mediate polyamine activation of the channel (Ahern et al., 2006). It emerges that the residues located on the vestibular surface of the pore are also important for channel activation. Consistent with the findings of Welch et al. (2000), we also observed that Glu636/Asp646 had a significant impact on channel opening. At 1 μM capsaicin, the wild-type channel exhibited bursts of openings separated by relatively long gaps, whereas the mutant D646N/E636Q displayed a noticeable reduction in the gap durations as well as the durations of the short closures within bursts, leading to an appearance of being almost constantly open. The ability of these residues to simultaneously influence conductance and gating suggests that the ion permeation and gating of the channel may be coupled. In further support of the notion, residues within the core of the pore have also been shown to affect channel gating. For example, the mutation M644Y in the putative filter causes the activation by capsaicin to be extremely slow (García-Martínez et al., 2000). The residue T633 on the pore helix is critical for proton activation; its mutation causes a selective ablation of low pH responses while leaving capsaicin and heat responses relatively intact (Ryu et al., 2007). Mutation of another pore helix residue, F640L, renders channels hypersensitive to thermal and chemical stimuli (Myers et al., 2008). Thus, the pore helix has functions beyond being a structural scaffold to support the selectivity filter. However, the mechanisms

of how these residues and those on the vestibular surface exert their functions remain unclear. The identification of possible interactions between Glu636 and Asp646 (as well as Lys639) suggests that the triad of the three charged residues in the region may be a pivotal component in support of the coupling between the pore helix and the vestibule/selectivity filter, thereby allowing for modulation of local conformations by environmental factors, such as low pH and cations.

We thank Dr. Charles Bowman for reading the manuscript.

This work was supported by National Institutes of Health grant R01-GM65994.

Paul J. De Weer served as editor.

Submitted: 4 May 2009
Accepted: 10 August 2009

REFERENCES

Ahern, G.P., I.M. Brooks, R.L. Miyares, and X.B. Wang. 2005. Extracellular cations sensitize and gate capsaicin receptor TRPV1 modulating pain signaling. *J. Neurosci.* 25:5109–5116.

Ahern, G.P., X. Wang, and R.L. Miyares. 2006. Polyamines are potent ligands for the capsaicin receptor TRPV1. *J. Biol. Chem.* 281:8991–8995.

Baumann, T.K., and M.E. Martenson. 2000. Extracellular protons both increase the activity and reduce the conductance of capsaicin-gated channels. *J. Neurosci.* 20:RC80.

Baumann, T.K., K.J. Burchiel, S.L. Ingram, and M.E. Martenson. 1996. Responses of adult human dorsal root ganglion neurons in culture to capsaicin and low pH. *Pain.* 65:31–38.

Begenisich, T., and M. Danko. 1983. Hydrogen ion block of the sodium pore in squid giant axons. *J. Gen. Physiol.* 82:599–618.

Bénitah, J.-P., J.R. Balser, E. Marban, and G.F. Tomaselli. 1997. Proton inhibition of sodium channels: mechanism of gating shifts and reduced conductance. *J. Membr. Biol.* 155:121–131.

Bernèche, S., and B. Roux. 2000. Molecular dynamics of the KcsA K(+) channel in a bilayer membrane. *Biophys. J.* 78:2900–2917.

Bernèche, S., and B. Roux. 2002. The ionization state and the conformation of Glu-71 in the KcsA K(+) channel. *Biophys. J.* 82:772–780.

Bevan, S., and J. Yeats. 1991. Protons activate a cation conductance in a sub-population of rat dorsal root ganglion neurones. *J. Physiol.* 433:145–161.

Bichet, D., F.A. Haass, and L.Y. Jan. 2003. Merging functional studies with structures of inward-rectifier K(+) channels. *Nat. Rev. Neurosci.* 4:957–967.

Brelidze, T.I., and K.L. Magleby. 2004. Protons block BK channels by competitive inhibition with K^+ and contribute to the limits of unitary currents at high voltages. *J. Gen. Physiol.* 123:305–319.

Bucher, D., L. Guidoni, and U. Rothlisberger. 2007. The protonation state of the Glu-71/Asp-80 residues in the KcsA potassium channel: a first-principles QM/MM molecular dynamics study. *Biophys. J.* 93:2315–2324.

Campbell, D.T. 1982. Do protons block Na+ channels by binding to a site outside the pore? *Nature.* 298:165–167.

Capener, C.E., P. Proks, F.M. Ashcroft, and M.S. Sansom. 2003. Filter flexibility in a mammalian K channel: models and simulations of Kir6.2 mutants. *Biophys. J.* 84:2345–2356.

Caterina, M.J., M.A. Schumacher, M. Tominaga, T.A. Rosen, J.D. Levine, and D. Julius. 1997. The capsaicin receptor: a heat-activated ion channel in the pain pathway. *Nature.* 389:816–824.

Caterina, M.J., A. Leffler, A.B. Malmberg, W.J. Martin, J. Trafton, K.R. Petersen-Zeitz, M. Koltzenburg, A.I. Basbaum, and D. Julius. 2000. Impaired nociception and pain sensation in mice lacking the capsaicin receptor. *Science.* 288:306–313.

Chen, C.C., S. England, A.N. Akopian, and J.N. Wood. 1998. A sensory neuron-specific, proton-gated ion channel. *Proc. Natl. Acad. Sci. USA.* 95:10240–10245.

Chen, X.H., I. Bezprozvanny, and R.W. Tsien. 1996. Molecular basis of proton block of L-type Ca2+ channels. *J. Gen. Physiol.* 108:363–374.

Chung, M.K., A.D. Güler, and M.J. Caterina. 2008. TRPV1 shows dynamic ionic selectivity during agonist stimulation. *Nat. Neurosci.* 11:555–564.

Cordero-Morales, J.F., L.G. Cuello, and E. Perozo. 2006. Voltage-dependent gating at the KcsA selectivity filter. *Nat. Struct. Mol. Biol.* 13:319–322.

Coulter, K.L., F. Périer, C.M. Radeke, and C.A. Vandenberg. 1995. Identification and molecular localization of a pH-sensing domain for the inward rectifier potassium channel HIR. *Neuron.* 15:1157–1168.

Daumas, P., and O.S. Andersen. 1993. Proton block of rat brain sodium channels. Evidence for two proton binding sites and multiple occupancy. *J. Gen. Physiol.* 101:27–43.

Davies, N.W., N.B. Standen, and P.R. Stanfield. 1992. The effect of intracellular pH on ATP-dependent potassium channels of frog skeletal muscle. *J. Physiol.* 445:549–568.

Davis, J.B., J. Gray, M.J. Gunthorpe, J.P. Hatcher, P.T. Davey, P. Overend, M.H. Harries, J. Latcham, C. Clapham, K. Atkinson, et al. 2000. Vanilloid receptor-1 is essential for inflammatory thermal hyperalgesia. *Nature.* 405:183–187.

Domene, C., A. Grottesi, and M.S. Sansom. 2004. Filter flexibility and distortion in a bacterial inward rectifier K+ channel: simulation studies of KirBac1.1. *Biophys. J.* 87:256–267.

Drouin, H., and B. Neumcke. 1974. Specific and unspecific charges at the sodium channels of the nerve membrane. *Pflugers Arch.* 351:207–229.

Garber, K. 2003. Why it hurts: researchers seek mechanisms of cancer pain. *J. Natl. Cancer Inst.* 95:770–772.

García-Martínez, C., C. Morenilla-Palao, R. Planells-Cases, J.M. Merino, and A. Ferrer-Montiel. 2000. Identification of an aspartic residue in the P-loop of the vanilloid receptor that modulates pore properties. *J. Biol. Chem.* 275:32552–32558.

Geiger, D., D. Becker, B. Lacombe, and R. Hedrich. 2002. Outer pore residues control the H(+) and K(+) sensitivity of the Arabidopsis potassium channel AKT3. *Plant Cell.* 14:1859–1868.

Hellwig, N., T.D. Plant, W. Janson, M. Schäfer, G. Schultz, and M. Schaefer. 2004. TRPV1 acts as proton channel to induce acidification in nociceptive neurons. *J. Biol. Chem.* 279:34553–34561.

Hui, K.Y., B.Y. Liu, and F. Qin. 2003. Capsaicin activation of the pain receptor, VR1: multiple open states from both partial and full binding. *Biophys. J.* 84:2957–2968.

Issberner, U., P.W. Reeh, and K.H. Steen. 1996. Pain due to tissue acidosis: a mechanism for inflammatory and ischemic myalgia? *Neurosci. Lett.* 208:191–194.

Jones, N.G., R. Slater, H. Cadiou, P. McNaughton, and S.B. McMahon. 2004. Acid-induced pain and its modulation in humans. *J. Neurosci.* 24:10974–10979.

Jordt, S.E., M. Tominaga, and D. Julius. 2000. Acid potentiation of the capsaicin receptor determined by a key extracellular site. *Proc. Natl. Acad. Sci. USA.* 97:8134–8139.

Kiss, L., J. LoTurco, and S.J. Korn. 1999. Contribution of the selectivity filter to inactivation in potassium channels. *Biophys. J.* 76:253–263.

Klöckner, U., and G. Isenberg. 1994. Intracellular pH modulates the availability of vascular L-type Ca2+ channels. *J. Gen. Physiol.* 103:647–663.

Kress, M., S. Fetzer, P.W. Reeh, and L. Vyklicky. 1996. Low pH facilitates capsaicin responses in isolated sensory neurons of the rat. *Neurosci. Lett.* 211:5–8.

Krishtal, O.A., and V.I. Pidoplichko. 1981. Receptor for protons in the membrane of sensory neurons. *Brain Res.* 214:150–154.

Liu, B., and F. Qin. 2005. Functional control of cold- and menthol-sensitive TRPM8 ion channels by phosphatidylinositol 4,5-bisphosphate. *J. Neurosci.* 25:1674–1681.

Liu, B., W. Ma, S. Ryu, and F. Qin. 2004. Inhibitory modulation of distal C-terminal on protein kinase C-dependent phospho-regulation of rat TRPV1 receptors. *J. Physiol.* 560:627–638.

Liu, Y., M.E. Jurman, and G. Yellen. 1996. Dynamic rearrangement of the outer mouth of a K+ channel during gating. *Neuron.* 16:859–867.

Loboda, A., A. Melishchuk, and C. Armstrong. 2001. Dilated and defunct K channels in the absence of K+. *Biophys. J.* 80:2704–2714.

Lopes, C.M., P.G. Gallagher, M.E. Buck, M.H. Butler, and S.A. Goldstein. 2000. Proton block and voltage gating are potassium-dependent in the cardiac leak channel Kcnk3. *J. Biol. Chem.* 275:16969–16978.

Lu, T., A.Y. Ting, J. Mainland, L.Y. Jan, P.G. Schultz, and J. Yang. 2001. Probing ion permeation and gating in a K+ channel with backbone mutations in the selectivity filter. *Nat. Neurosci.* 4:239–246.

Martenson, M.E., S.L. Ingram, and T.K. Baumann. 1994. Potentiation of rabbit trigeminal responses to capsaicin in a low pH environment. *Brain Res.* 651:143–147.

Morrill, J.A., and R. MacKinnon. 1999. Isolation of a single carboxyl-carboxylate proton binding site in the pore of a cyclic nucleotide-gated channel. *J. Gen. Physiol.* 114:71–83.

Myers, B.R., C.J. Bohlen, and D. Julius. 2008. A yeast genetic screen reveals a critical role for the pore helix domain in TRP channel gating. *Neuron.* 58:362–373.

Nimigean, C.M., J.S. Chappie, and C. Miller. 2003. Electrostatic tuning of ion conductance in potassium channels. *Biochemistry.* 42:9263–9268.

Ohta, T., T. Imagawa, and S. Ito. 2008. Novel gating and sensitizing mechanism of capsaicin receptor (TRPV1): tonic inhibitory regulation of extracellular sodium through the external protonation sites on TRPV1. *J. Biol. Chem.* 283:9377–9387.

Pan, H.L., J.C. Longhurst, J.C. Eisenach, and S.R. Chen. 1999. Role of protons in activation of cardiac sympathetic C-fibre afferents during ischaemia in cats. *J. Physiol.* 518:857–866.

Petersen, M., and R.H. LaMotte. 1993. Effect of protons on the inward current evoked by capsaicin in isolated dorsal root ganglion cells. *Pain.* 54:37–42.

Proks, P., C.E. Capener, P. Jones, and F.M. Ashcroft. 2001. Mutations within the P-loop of Kir6.2 modulate the intraburst kinetics of the ATP-sensitive potassium channel. *J. Gen. Physiol.* 118:341–353.

Ranatunga, K.M., I.H. Shrivastava, G.R. Smith, and M.S. Sansom. 2001. Side-chain ionization states in a potassium channel. *Biophys. J.* 80:1210–1219.

Root, M.J., and R. MacKinnon. 1994. Two identical noninteracting sites in an ion channel revealed by proton transfer. *Science.* 265:1852–1856.

Rosenbaum, T., M. Awaya, and S.E. Gordon. 2002. Subunit modification and association in VR1 ion channels. *BMC Neurosci.* 3:4.

Ryu, S., B. Liu, and F. Qin. 2003. Low pH potentiates both capsaicin binding and channel gating of VR1 receptors. *J. Gen. Physiol.* 122:45–61.

Ryu, S., B. Liu, J. Yao, Q. Fu, and F. Qin. 2007. Uncoupling proton activation of vanilloid receptor TRPV1. *J. Neurosci.* 27:12797–12807.

Samways, D.S., B.S. Khakh, and T.M. Egan. 2008. Tunable calcium current through TRPV1 receptor channels. *J. Biol. Chem.* 283:31274–31278.

Starkus, J.G., L. Kuschel, M.D. Rayner, and S.H. Heinemann. 1997. Ion conduction through C-type inactivated Shaker channels. *J. Gen. Physiol.* 110:539–550.

Steen, K.H., and P.W. Reeh. 1993. Sustained graded pain and hyperalgesia from harmless experimental tissue acidosis in human skin. *Neurosci. Lett.* 154:113–116.

Steen, K.H., A.E. Steen, H.W. Kreysel, and P.W. Reeh. 1996. Inflammatory mediators potentiate pain induced by experimental tissue acidosis. *Pain.* 66:163–170.

Stoop, R., A. Surprenant, and R.A. North. 1997. Different sensitivities to pH of ATP-induced currents at four cloned P2X receptors. *J. Neurophysiol.* 78:1837–1840.

Sutherland, S.P., C.J. Benson, J.P. Adelman, and E.W. McCleskey. 2001. Acid-sensing ion channel 3 matches the acid-gated current in cardiac ischemia-sensing neurons. *Proc. Natl. Acad. Sci. USA.* 98:711–716.

Tominaga, M., M.J. Caterina, A.B. Malmberg, T.A. Rosen, H. Gilbert, K. Skinner, B.E. Raumann, A.I. Basbaum, and D. Julius. 1998. The cloned capsaicin receptor integrates multiple pain-producing stimuli. *Neuron.* 21:531–543.

Tytgat, J., B. Nilius, and E. Carmeliet. 1990. Modulation of the T-type cardiac Ca channel by changes in proton concentration. *J. Gen. Physiol.* 96:973–990.

Ugawa, S., T. Ueda, Y. Ishida, M. Nishigaki, Y. Shibata, and S. Shimada. 2002. Amiloride-blockable acid-sensing ion channels are leading acid sensors expressed in human nociceptors. *J. Clin. Invest.* 110:1185–1190.

Waldmann, R., G. Champigny, F. Bassilana, C. Heurteaux, and M. Lazdunski. 1997. A proton-gated cation channel involved in acid-sensing. *Nature.* 386:173–177.

Welch, J.M., S.A. Simon, and P.H. Reinhart. 2000. The activation mechanism of rat vanilloid receptor 1 by capsaicin involves the pore domain and differs from the activation by either acid or heat. *Proc. Natl. Acad. Sci. USA.* 97:13889–13894.

Woodhull, A.M. 1973. Ionic blockage of sodium channels in nerve. *J. Gen. Physiol.* 61:687–708.

Xu, H., Z. Yang, N. Cui, S. Chanchevalap, W.W. Valesky, and C. Jiang. 2000. A single residue contributes to the difference between Kir4.1 and Kir1.1 channels in pH sensitivity, rectification and single channel conductance. *J. Physiol.* 528:267–277.

Yao, J., and F. Qin. 2009. Interaction with phosphoinositides confers adaptation onto the TRPV1 pain receptor. *PLoS Biol.* 7:e46.

Yifrach, O. 2004. Hill coefficient for estimating the magnitude of cooperativity in gating transitions of voltage-dependent ion channels. *Biophys. J.* 87:822–830.

Zhang, J.F., and S.A. Siegelbaum. 1991. Effects of external protons on single cardiac sodium channels from guinea pig ventricular myocytes. *J. Gen. Physiol.* 98:1065–1083.

Zheng, J., and F.J. Sigworth. 1997. Selectivity changes during activation of mutant Shaker potassium channels. *J. Gen. Physiol.* 110:101–117.

Zhou, Y., and R. MacKinnon. 2003. The occupancy of ions in the K+ selectivity filter: charge balance and coupling of ion binding to a protein conformational change underlie high conduction rates. *J. Mol. Biol.* 333:965–975.

Zhou, Y., J.H. Morais-Cabral, A. Kaufman, and R. MacKinnon. 2001. Chemistry of ion coordination and hydration revealed by a K+ channel-Fab complex at 2.0 A resolution. *Nature.* 414:43–48.